Kinetics and Equilibrium of Barium and Strontium Sulfate Formation in Marcellus Shale Flowback Water

Can He[1]; Meng Li[2]; Wenshi Liu[3]; Elise Barbot[4]; and Radisav D. Vidic, M.ASCE[5]

Abstract: Flowback water from natural gas extraction in Marcellus Shale contains very high concentrations of inorganic salts and organic chemicals. Potential reuse of this water in subsequent hydraulic-fracturing operations may be limited by high concentrations of divalent cations (e.g., Ba, Sr, and Ca). Kinetics of barite and celestite precipitation in flowback waters from different well sites was evaluated in this study. Ba reacted rapidly with sulfate and reached equilibrium within 30 min, whereas Sr reacted slowly and took days to reach equilibrium. Equilibrium concentrations of Ba and Sr predicted by thermodynamics models were compared with experimental results. Activity corrections based on the Pitzer equation provided the best agreement with experimental data for both Ba and Sr. Comparison of barite and celestite precipitation kinetics in actual and synthetic flowback water revealed that there was no observable impact of organics and other minor components in actual flowback water on barite precipitation rate. This was primarily due to the fact that barite precipitation occurred relatively quickly at the high saturation levels utilized in this study. By contrast, lattice poisoning and complexation with organic matter had a profound impact on the comparatively slower celestite precipitation. The presence of organic matter in actual flowback water increased Ba and Sr concentrations in solution, and contributed to the discrepancy between measured and predicted equilibrium concentrations.
DOI: 10.1061/(ASCE)EE.1943-7870.0000807.

Author keywords: Chemical precipitation; Barite; Celestite; Kinetics; Thermodynamic predictions; Shale gas.

Introduction

Development of unconventional on-shore reservoirs is a growing source of natural gas to meet the energy needs of the United States. Recent advances in horizontal drilling and multistage hydraulic-fracturing technologies have enabled development of highly productive gas wells in Marcellus Shale (Harper 2008). The Marcellus Shale of the Appalachian Basin has recently been estimated to contain 262–500 Tcf (trillion cubic feet) of natural gas reserves, and is one of the largest underdeveloped reservoirs of shale gas in the U.S. (Engelder and Lash 2008; Milici and Swezey 2006). Marcellus Shale underlies approximately 70% of Pennsylvania (de Witt 1993) and contains natural gas reserves that could supply the eastern U.S. for many years (Pletcher 2008).

Hydraulic fracturing (hydrofracking) is the cornerstone technology that has enabled economical recovery of natural gas from Marcellus Shale. It involves the introduction of fracturing fluid at high pressure to enlarge existing fractures or to make new fractures in the shale formation, thereby increasing its permeability to enable economical gas recovery rates. The fracturing fluid contains freshwater withdrawn from local streams that is amended with chemical additives, including (1) friction reducers to optimize flow characteristics, (2) biocides to inhibit biological growth, (3) proppant material, such as well-sorted sand, to hold the fractures open, (4) corrosion inhibitors to protect well casing, (5) scale inhibitors to preserve the permeability of the proppant pack and the formation, and (6) surfactants to aid in fluid recovery (Economides et al. 1998; Vidic et al. 2013). Hydrofracturing a single Marcellus well may require 3–5 million gallons of fracturing fluid (Rodgers 2008), of which 10–40% may return to the surface as flowback water (Harper 2008).

Natural gas developers bear considerable cost to purchase fresh water, transport fresh water to a site, and transport contaminated flowback and produced water to a disposal/treatment site where they also pay for its disposal. As a result, a variety of solutions for recycling flowback water and its reuse in hydraulic fracturing have been developed recently (Vidic et al. 2013). This approach reduces the cost of natural gas production, especially in areas where fresh water is scarce and/or disposal costs are high.

The flowback and produced water contains inorganic salts, metals, and organics from the target geologic formation; it exhibits vastly different chemistry than the original fracturing fluid. Once brought to the surface, this water must be managed in accordance with federal, state, and local environmental regulations. Water-management options are severely limited by the unusually high concentration of chemical constituents (Hill et al. 2004) and the high-volume flow observed during the flowback period. Total dissolved solids in flowback and produced water from Marcellus Shale are high enough to cause a concern for its reuse, particularly because of high concentrations of Ba and Sr that may precipitate in the well or in the formation.

[1]Graduate Research Assistant, Dept. of Civil and Environment Engineering, Univ. of Pittsburgh, 3700 O'Hara St., Pittsburgh, PA 15261. E-mail: cah162@pitt.edu

[2]Graduate Research Assistant, Dept. of Civil and Environment Engineering, Univ. of Pittsburgh, 3700 O'Hara St., Pittsburgh, PA 15261. E-mail: ibmirie@gmail.com

[3]Ph.D. Candidate, Dept. of Civil and Environment Engineering, Univ. of Pittsburgh, 3700 O'Hara St., Pittsburgh, PA 15261. E-mail: wel44@pitt.edu

[4]Postdoctoral Researcher, Dept. of Civil and Environment Engineering, Univ. of Pittsburgh, 3700 O'Hara St., Pittsburgh, PA 15261. E-mail: elisebarbot@gmail.com

[5]William Kepler Whiteford Professor, Dept. of Civil and Environment Engineering, Univ. of Pittsburgh, 3700 O'Hara St., Pittsburgh, PA 15261 (corresponding author). E-mail: vidic@pitt.edu

Note. This manuscript was submitted on February 22, 2013; approved on November 14, 2013; published online on January 10, 2014. Discussion period open until June 10, 2014; separate discussions must be submitted for individual papers. This paper is part of the ***Journal of Environmental Engineering***, © ASCE, ISSN 0733-9372/B4014001(9)/$25.00.

It is well known that Ba and Sr can be removed from solution through precipitation as sulfate salts. However, it is not known whether equilibrium predictions typically available for fairly dilute solutions would still be applicable under the extremely high ionic strength conditions that are typical of Marcellus-Shale flowback water. This study focused on the applicability of chemical-equilibrium models to predict Ba and Sr behavior in synthetic and actual Marcellus-Shale flowback water upon sulfate addition, which is a common practice in centralized waste-treatment facilities used for flowback/produced water purification before reuse in hydraulic fracturing.

Materials and Methods

Flowback Water Characteristics

The chemical composition of flowback water varies with location and well-completion practice (Barbot et al. 2013). Flowback water samples used in this study came from three Marcellus wells located in southwest Pennsylvania, which are designated as Site A, Site B, and Site C. The key characteristics of the flow-composite water samples used in this study are shown in Table 1. In general, they are all concentrated brines with ionic strengths ranging from 0.91 to 3.41 M. Sodium, calcium, barium, and strontium are the major cations, whereas chloride is the major anion in Marcellus-Shale flowback water. The flowback water from Site A is characterized by low Ba and Sr concentrations and medium Ca content; Site B has high Ba and Sr concentrations but low Ca content; and Site C has very low Ba concentration but very high Sr and Ca contents.

Experimental Protocol

The synthetic flowback water samples were prepared in 1-L volumetric flasks using high-purity chemicals. Synthetic or actual flowback water was placed in 250-mL volumetric flasks, and sulfate was added as anhydrous $NaSO_4$ (J. T. Baker, Phillipsburg, NJ) to simulate the treatment process in centralized wastewater-treatment plants in Pennsylvania. Solutions were mixed with magnetic bar at 400 rpm, and samples were taken at predetermined time intervals and filtered through 0.45-μm nylon filters. Ba and Sr were measured using an atomic adsorption spectrometer (Perkin-Elmer model 1000 AAS) with a nitrous oxide-acetylene flame. To eliminate the interference from ionization and retard the kinetics of precipitation reactions, all filtered samples were immediately diluted with 0.15% KCl and 2% HNO_3 solutions [EPA method 208.1 (EPA 1974); Agilent Technology, Inc 2010]. Analysis for each cation was performed at least three times, and the average value was used if the standard deviation was less than 10%.

Table 1. Key Inorganic Constituents of Flowback Water Used in This Study (mg/L)

Constituent	Site A	Site B	Site C
Na^+	16,518	32,327.8	46,130.7
Ca^{2+}	2,224	449.1	15,021
Mg^{2+}	220	119.9	1,720
Ba^{2+}	730	2,530	236
Sr^{2+}	367	1,387	1,817
Cl^-	29,000	52,913.5	104,300
Ionic strength (M)	0.91	1.55	3.41

Chemical-Equilibrium Models

MINEQL+ (Westall et al. 1976) and PhreeqcI (Parkhurst and Appelo 1999) were used to calculate the equilibrium distributions for the ions of interest (i.e., Ba^{2+} and Sr^{2+}). MINEQL+ uses the Davis equation (Davis 1962) to calculate activity coefficients, whereas the PhreeqcI software package allows selection between the "Wateq" Debye-Hückel equation (Truesdell and Jones 1974) and the Pitzer equation (Pitzer 1973, 1991).

Because of the high ionic strength of flowback water, it is important to accurately estimate activity coefficients of different components and species that may be involved in the chemical reactions of interest. The Davis equation is valid for ionic strength (I) less than 0.5 and is defined as follows:

$$\log(\gamma_i) = -A \cdot Z_i^2 \left(\frac{\sqrt{I}}{1+\sqrt{I}} - 0.2I \right) \quad (1)$$

The Wateq Debye-Hückel model is valid for $I < 1$ and is defined as follows:

$$\log(\gamma_i) = \frac{-A \cdot Z_i^2 \cdot \sqrt{I}}{1 + B \cdot a_i \cdot \sqrt{I}} + b_i \cdot I \quad (2)$$

where $A = (1.82483 \cdot 10^6 \sqrt{d})/(\varepsilon \cdot T_k)^{3/2}$ and $B = (50.2916\sqrt{d})/(\varepsilon \cdot T_k)^{1/2}$ (Merkel and Planer-Friedrich 2008); a_i and b_i are ion-specific parameters determined by the ion size (Table 2); d = density of water; ε = dielectric constant; T_K = temperature in Kelvin; and I = ionic strength.

Another semiempirical model based on ion-interaction theory was developed for high ionic strength conditions (Pitzer 1973). Compared to ion-association theory or ion-pair theory, the ion-interaction model considers all charged ions to be fully separated as free ions. This model was later edited (Pitzer 1991) to incorporate the ion-association model and solve some inaccuracies for weak electrolytes. The general equations used for calculating the activity coefficient by Pitzer equations for cations and anions are listed as follows (Aniceto et al. 2012) :

Table 2. Ion-Specific Parameters a_i and b_i Based on Parkhurst et al. (1980) and Truesdell and Jones (1974)

Ion	a_i (Å)	b_i (Å)
H^+	4.78	0.24
Li^+	4.76	0.20
Na^+	4.32	0.06
K^+	3.71	0.01
Cs^{2+}	1.81	0.01
Mg^{2+}	5.46	0.22
Ca^{2+}	4.86	0.15
Sr^{2+}	5.48	0.11
Ba^{2+}	4.55	0.09
Al^{3+}	6.65	0.19
Mn^{2+}	7.04	0.22
Fe^{2+}	5.08	0.16
Co^{2+}	6.17	0.22
Ni^{2+}	5.51	0.22
Zn^{2+}	4.87	0.24
Cd^{2+}	5.80	0.10
Pb^{2+}	4.80	0.01
OH^-	10.65	0.21
F^-	3.46	0.08
Cl^-	3.71	0.01
ClO_4^-	5.30	0.08
SO_4^{2-}	5.31	−0.07

$$\ln \gamma_M = z_M^2 F + \sum_a m_a \left[2B_{Ma} + \left(2\sum_c m_c z_c \right) C_{Ma} \right] + \sum_c m_c \left(2\emptyset_{Mc} + \sum_a m_a \Psi_{Mca} \right) + \frac{1}{2} \sum_a \sum_{<a'} m_a m_a' \Psi_{Maa'} + \sum_c \sum_a m_c m_a (z_M^2 B_{ij}' + |z_M| C_{ca}) \quad (3)$$

$$\ln \gamma_X = z_X^2 F + \sum_c m_c \left[2B_{cX} + \left(2\sum_a m_a z_a \right) C_{cX} \right] + \sum_a m_a \left(2\emptyset_{cX} + \sum_c m_c \Psi_{Xca} \right) + \frac{1}{2} \sum_c \sum_{<c'} m_c m_{c'} \Psi_{Xcc'} + \sum_c \sum_a m_c m_a (z_X^2 B_{ij}' + |z_X| C_{ca}) \quad (4)$$

where subscripts M and X denote cation and anion of interest, respectively; subscripts c and a indicate other cations and anions; and F is a derived Debye-Hückel function, which is dependent on the Debye-Hückel parameter A and ionic strength. Other terms in these equations are determined based on six types of temperature-dependent empirical parameters [i.e., $\beta_{MX}^{(0)}$, $\beta_{MX}^{(1)}$, $\beta_{MX}^{(2)}$, $C_{MX}^{(0)}$, Φ_{ij}, Ψ_{ijk}]. The first three terms [namely, $\beta_{MX}^{(0)}$, $\beta_{MX}^{(1)}$, $\beta_{MX}^{(2)}$] describe the interaction of oppositely charged ion pairs in a mixed electrolyte solution. $C_{MX}^{(0)}$ accounts for short-range ion interaction and is of importance at high concentrations. Φ_{ij} are mixed electrolyte parameters for interaction between ions of the same charge, and Ψ_{ijk} describe cation-cation-anion and anion-anion-cation interactions in a mixed-electrolyte solution (Pitzer and Mayorga 1973; Pitzer and Kim 1974; Pitzer 1975, 1991). Table 3 lists empirical parameters that were used to supplement the database available in PhreeqcI.

The Pitzer equation is preferred over other models for two reasons. First, the Pitzer equation is applicable for solutions with ionic strength up to 6 M (Burkin 2001). Second, the Pitzer equation takes into account the impact of all ions that are present in solution, which means that the activity coefficients will vary with dissolved ion composition for identical ionic strength.

Table 3. Ionic Interaction Parameters in the Pitzer Equation

Parameter	Value	Reference
$\beta^{(0)}$ Ba-SO_4	−1.0	Monnin and Galinier (1988)
$\beta^{(0)}$ Sr-SO_4	−0.43	Monnin and Galinier (1988)
$\beta^{(0)}$ Mg-SO_4	0.221	Pabalan and Pitzer (1987)
$\beta^{(0)}$ Ca-SO_4	0.2	Greenberg and Moller (1989)
$\beta^{(1)}$ Ba-SO_4	12.6	Monnin and Galinier (1988)
$\beta^{(1)}$ Sr-SO_4	5.7	Monnin and Galinier (1988)
$\beta^{(1)}$ Mg-SO_4	3.343	Harvie et al. (1984)
$\beta^{(1)}$ Ca-SO_4	3.1973	Greenberg and Moller (1989)
$\beta^{(2)}$ Ba-SO_4	−153.4	Monnin and Galinier (1988)
$\beta^{(2)}$ Sr-SO_4	−94.2	Monnin and Galinier (1988)
$\beta^{(2)}$ Mg-SO_4	−37.23	Pabalan and Pitzer (1987)
$\beta^{(2)}$ Ca-SO_4	−54.24	Greenberg and Moller (1989)
Ψ Na-Ca-Cl	−0.003	Holmes et al. (1987)
Ψ Na-Ca-SO_4	−0.012	Greenberg and Moller (1989)
Ψ Na-Ba-Cl	0.0128	Monnin (1999)
Ψ Cl-SO_4-Mg	−0.008	Harvie et al. (1984)
Φ SO_4-Cl	0.07	Greenberg and Moller (1989)

Results and Discussion

Kinetics of Barite and Celestite Precipitation in Synthetic Flowback Waters

Previous studies (He et al. 1995a, b; Risthaus et al. 2001; Jones et al. 2004; Shen et al. 2009; Fan et al. 2011) have shown that a number of parameters, including temperature, pressure, saturation index, ionic strength, and scale inhibitors, have significant impact on the kinetics of barite and celestite precipitation. In this study, the temperature and pressure were at standard conditions (atmospheric pressure and room temperature of 22 ± 1°C), and the focus was on the impact of water quality on these reactions. Mineral precipitation involves two stages: nucleation and crystal growth. The initiation of precipitation reactions is accomplished during the induction period, which depends on the saturation index, and is usually completed within a couple of minutes (He et al. 1995a, b; Fan et al. 2011). However, the equilibrium will take much longer to achieve, and the precipitation rate normally follows a second-order reaction rate (Yeboah et al. 1994; Shen et al. 2008). The study by Shen et al. (2008) found that barite precipitation reaches equilibrium fairly quickly when the reaction goes from undersaturation to saturation,

Table 4. Initial Concentrations of Ba^{2+}, Sr^{2+}, and SO_4^{2-} in Synthetic Flowback Waters and Corresponding Ionic Strength, Activities, and Saturation Indices with Respect to Barite and Celestite

Flowback water	$[SO_4^{2-}]$ (mg/L)	$[Ba^{2+}]$ (mg/L)	$[Sr^{2+}]$ (mg/L)	Ionic strength (IS) (mol)	α_{SO4} (mol/L) × 10^3	α_{Ba} (mol/L) × 10^3	α_{Sr} (mol/L) × 10^3	SI_{BaSO4}	SI_{SrSO4}
Site A	1,000	730	367	0.95	0.781	1.115	1.051	3.91	0.55
	2,000	730	367	0.98	1.542	1.126	1.106	4.21	0.83
	3,000	730	367	1.02	2.284	1.139	0.985	4.39	0.98
Site B	1,000	2,530	1,387	1.64	0.559	3.763	4.396	4.29	1.03
	2,000	2,530	1,387	1.68	1.104	3.830	4.309	4.60	1.31
	3,000	2,530	1,387	1.71	1.637	3.898	4.227	4.78	1.48
Site C	150	236	1,817	3.62	0.029	0.568	11.65	2.20	0.18
	500	236	1,817	3.63	0.098	0.572	11.63	2.72	0.70
	1,000	236	1,817	3.65	0.197	0.577	11.59	3.03	1.00

Note: SI = saturation index, the logarithm of Ω (Ω is the ratio of IAP/K_{sp}, where IAP = ion activity product); $K_{sp,BaSO4} = 1.072 \times 10^{-10}$, $K_{sp,SrSO4} = 2.291 \times 10^{-7}$.

whereas the rate becomes relatively slow if the direction is from supersaturation to saturation. The focus of this study was on the latter case, because the reacting ions always initially exceed the saturation levels in practice.

A summary of experimental conditions, including the initial ion concentrations, ionic strength of the solution, ion activities calculated using the Pitzer equation, and saturation indices, is given in Table 4. Visual observations in almost all tests conducted in this study revealed significant turbidity development within a few seconds of sulfate addition, which indicates a relatively short induction period, and barium-sulfate nucleation that is much faster than the nucleation rates found in other studies (He et al. 1995a, b; Fan et al. 2011). Hence, the induction period was not evaluated further in this study.

Figs. 1 and 2 depict variations of Ba and Sr in three flowback water samples with time for different $NaSO_4$ doses. As evidenced from these figures, barite precipitated much faster than celestite in all cases. The difference in time required to achieve equilibrium for Ba and Sr was very significant for flowback samples from Sites A and B, in which Ba precipitation was essentially complete within 30 min, whereas Sr concentration did not stabilize after 24 h, and weeks may be needed to achieve equilibrium (data not shown). As shown in Table 4, the saturation index (SI) for barite ($2.2 \sim 4.8$) was much higher than that for celestite ($0.18 \sim 1.48$). Jones et al. (2004) suggested that the concentrations of other divalent ions, especially Ca, may impact barite and celestite precipitation kinetics by lattice poisoning. However, inhibition of barite precipitation was only observed in the case of flowback water from Site C with addition of 150 mg/L SO_4 [Fig. 1(c), (initial SI = 2.2)], which suggests that the inhibition of barite precipitation by Na and Ca ions only occurs when the barite saturation index is low. In such cases, it is necessary to increase SO_4 dosage (e.g., achieve initial SI greater than 2.5) to ensure rapid barite precipitation.

The Sr concentration in the presence of relatively low initial sulfate concentration exhibited slightly unusual behavior. When 150 mg/L of sulfate was added to flowback sample from Site C [Fig. 2(c)], Sr concentration in solution initially decreased and then increased over time. Such behavior can be explained by the nucleation kinetics model for a binary system [i.e., $(Ba, Sr)SO_4$] suggested by Pina and Putnis (2002). Sr and Ba are initially coprecipitated in the form of $Ba_xSr_{1-x}SO_4$. This initial coprecipitation step proceeds on the basis of the kinetically favored pattern, which is governed by the molar faction of Ba in the coprecipitated solid (i.e., x in $Ba_xSr_{1-x}SO_4$). When the ratio of strontium to barium in solution is high, as is the case in flowback water from Site C, relatively Sr-rich solid composition can be expected initially as a large fraction of sulfate is initially consumed for celestite formation. However, Sr is then replaced with Ba through isomorphic substitution because the equilibrium is ultimately driven by supersaturation, which is much higher for barite than for celestite. Isomorphic

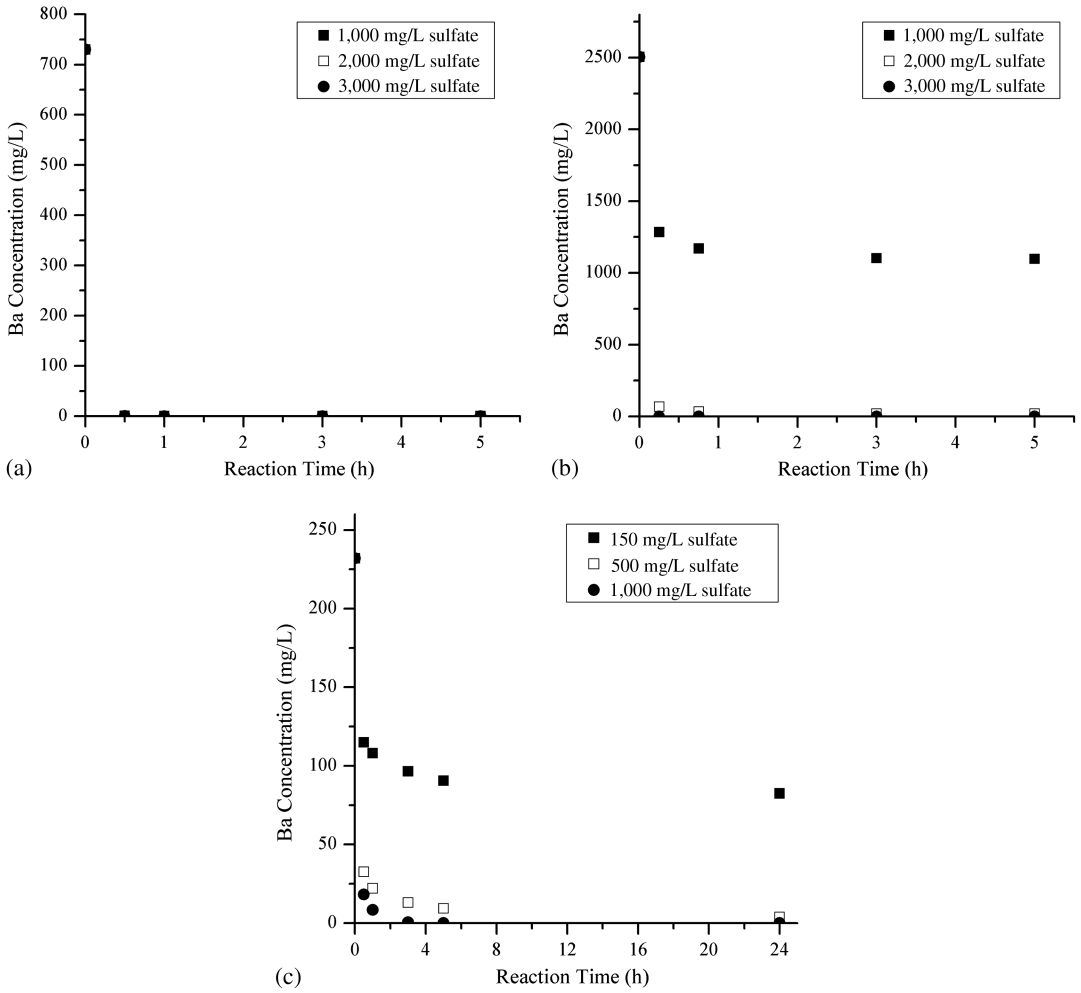

Fig. 1. Variation of Ba concentration for different initial sulfate concentrations in flowback water from: (a) Site A; (b) Site B; (c) Site C. Barite precipitation is essentially complete in 30 min if the initial SI > 2.5 regardless of the solution composition

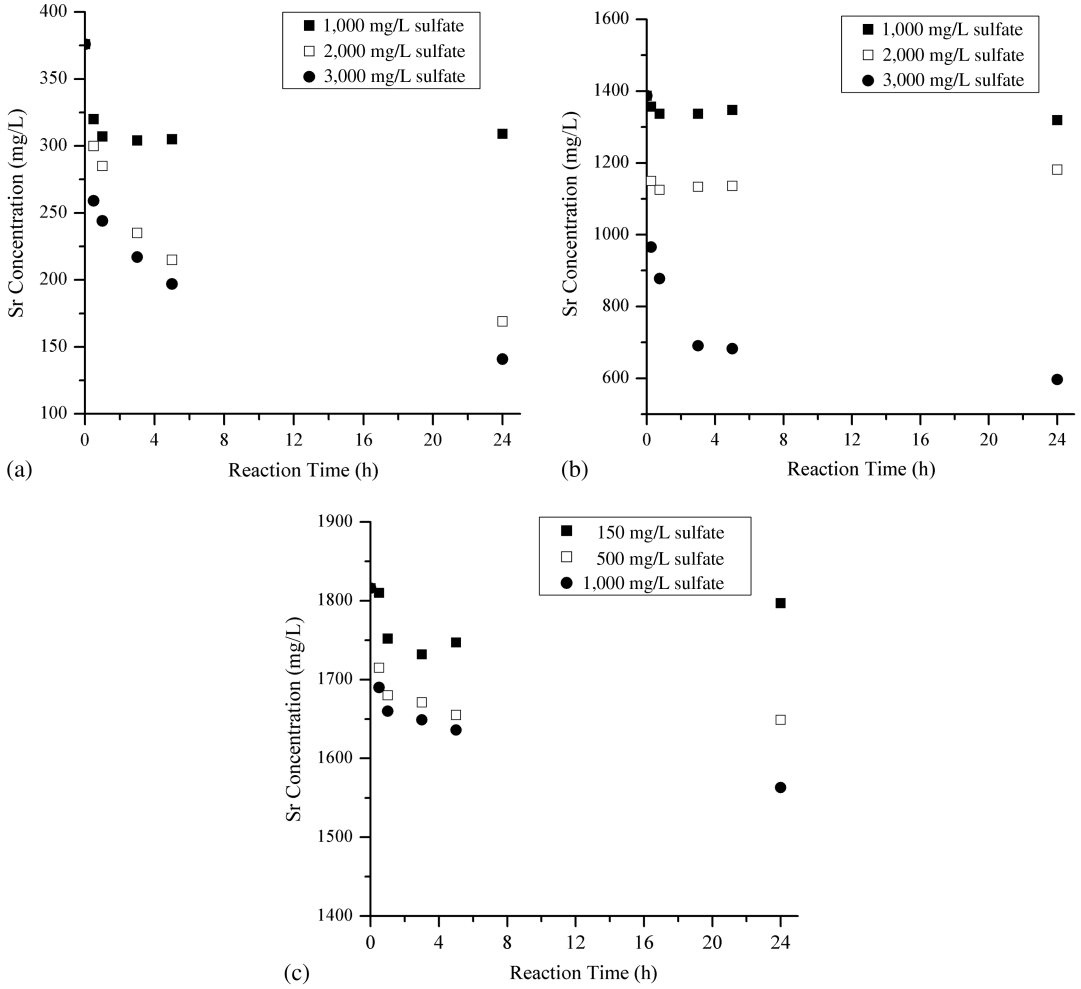

Fig. 2. Variation of Sr concentration for different initial sulfate concentrations in flowback water from: (a) Site A; (b) Site B; (c) Site C. Low SI for celestite results in relatively slow precipitation reactions

substitution is a fairly slow process, and Ba did not reach equilibrium even after 30 days (data not shown).

Table 5 shows that the removal efficiency for Ba would be much higher than that for Sr under typical process conditions in centralized waste-treatment facilities (e.g., reaction time of 1 h). Sulfate is an excellent removal reagent for Ba, but not as good at removing Sr, because barite solubility is approximately three orders of magnitude lower than that of celestite, and very high initial sulfate concentrations would be required to achieve significant Sr removal.

Table 5. Measured Removal Efficiency of Ba^{2+} and Sr^{2+} in Synthetic Flowback Waters after 1 h Reaction for Different Initial Sulfate Concentrations

Mixtures	Ba removal efficiency (%)	Sr removal efficiency (%)
Site A + 1,000 mg/L SO_4	100.0	18.4
Site A + 2,000 mg/L SO_4	100.0	24.2
Site A + 3,000 mg/L SO_4	100.0	35.1
Site B + 1,000 mg/L SO_4	53.3	3.6
Site B + 2,000 mg/L SO_4	98.6	18.3
Site B + 3,000 mg/L SO_4	100.0	36.7
Site C + 150 mg/L SO_4	55.6	3.5
Site C + 500 mg/L SO_4	90.5	8.6
Site C + 1,000 mg/L SO_4	96.4	10.1

However, this approach would lead to substantial increase in sulfate concentration in the finished water, which could prevent the reuse of this water for hydraulic fracturing because of concerns that sulfate precipitation inside the well could reduce well productivity. If high Sr removal is needed, it may be better to precipitate it as strontium carbonate (strontianite), which has much lower solubility ($K_{sp,SrCO3} = 10^{-9.25}$) than that of celestite (Miller and Benson 1983).

Equilibrium Predictions for Synthetic Flowback Waters

Experimental data collected using synthetic flowback water from Site A (IS = 0.91M), Site B (IS = 1.55M), and Site C (IS = 3.41M) are compared to chemical-equilibrium predictions for different initial sulfate concentrations in Figs. 3–5, respectively. These figures show that the theoretical calculations are in good agreement with experimental results for Ba, with the Pitzer equation offering the best predictions. One exception was in the case of Ba concentration in flowback water from Site C with an initial sulfate concentration of 150 mg/L [Fig. 5(a)]. The deviation between measured values and model predictions based on the Pitzer equation in this case is expected and can be explained by kinetic limitation (i.e., low SI for barite), lattice poisoning by high concentrations of cations in solution (I = 3.41), and slow isomorphic substitution (i.e., high initial $[Sr^{2+}]/[Ba^{2+}]$ ratio) as described previously.

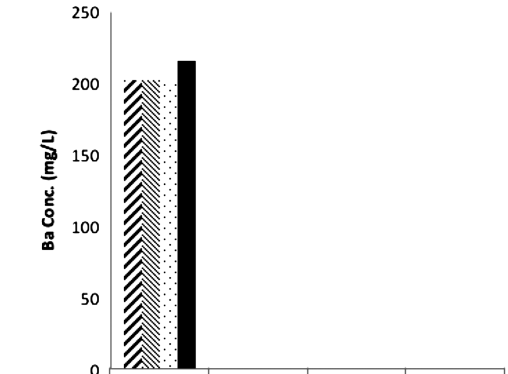

	400 mg/L sulfate	1,000 mg/L sulfate	2,000 mg/L sulfate	3,000 mg/L sulfate
Davis	202	0.17	0.05	0.03
Wateq	202	0.24	0.08	0.04
Pitzer	202	0.26	0.08	0.05
Measured	215	0.2	0	0

(a)

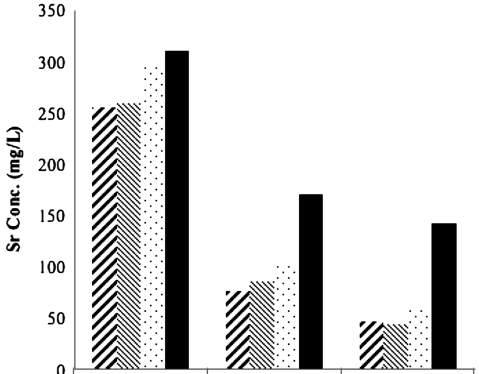

	1,000 mg/L sulfate	2,000 mg/L sulfate	3,000 mg/L sulfate
Davis	254	75.1	45.2
Wateq	259	85.2	42.8
Pitzer	297.6	99.9	57.3
Measured	309	169	141

(b)

Fig. 3. Comparison between equilibrium predictions and experimental results for different initial sulfate concentrations after 24 h of reaction in synthetic flowback water from Site A for (a) Ba; (b) Sr

In general, the chemical-equilibrium model using the Pitzer equation also offered the best match with experimental data for Sr collected in this study. The only significant deviation between measured and predicted Sr concentration was observed in the case when the initial Sr concentration was low (e.g., flowback water from Site A). Such behavior [Fig. 3(b)] can be explained by the fact that it can take several weeks to reach equilibrium with respect to celestite precipitation (data not shown). The prediction accuracy is improved when Sr concentration is relatively high (e.g., flowback water from Sites B and C), and it decreases with an increase in the initial sulfate concentration.

Comparison of Barite and Celestite Precipitation in Synthetic and Real Flowback Waters

The actual flowback water is a much more complex solution compared with the synthetic water that contains only salts. The presence of organic matter from either the rock formation or from the chemical additives injected into the fracturing fluid may have an impact on precipitation kinetics, equilibrium, and size and morphology of crystals that are formed. Whether the organic substances can inhibit or accelerate precipitation of inorganic compounds is still a matter of debate (Hennesy and Graham 2002; Jones et al. 2004, 2008; Smith et al. 2004; Hamdona et al. 2010). Most studies suggest that

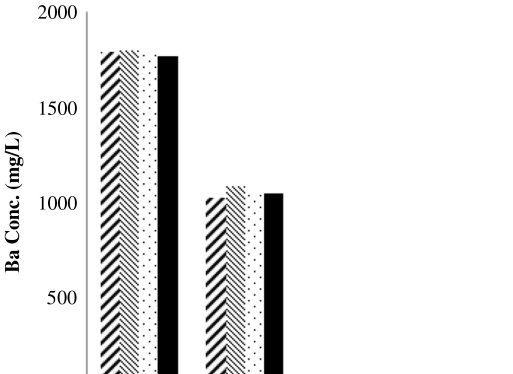

	500 mg/L sulfate	1,000 mg/L sulfate	2,000 mg/L sulfate	3,000 mg/L sulfate
Davis	1,785	1,016	0.8	0.26
Wateq	1,791	1,076	1.49	0.56
Pitzer	1,791	1,041	1.36	0.5
Measured	1,762	1,038	10.8	2.1

(a)

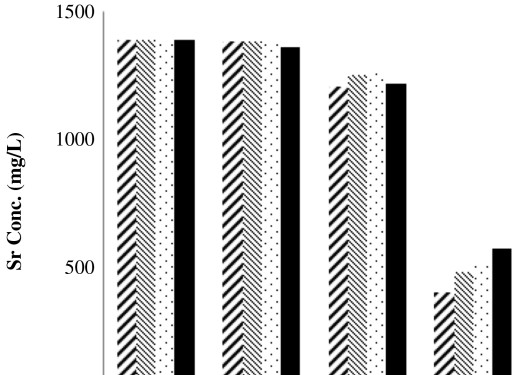

	500 mg/L sulfate	1,000 mg/L sulfate	2,000 mg/L sulfate	3,000 mg/L sulfate
Davis	1,387	1,376	1,200	386
Wateq	1,387	1,376	1,244	469
Pitzer	1,387	1,376	1,255	490
Measured	1,387	1,355	1,213	559

(b)

Fig. 4. Comparison between equilibrium predictions and experimental results for different initial sulfate concentrations after 48 h of reaction in synthetic flowback water from Site B for (a) Ba; (b) Sr

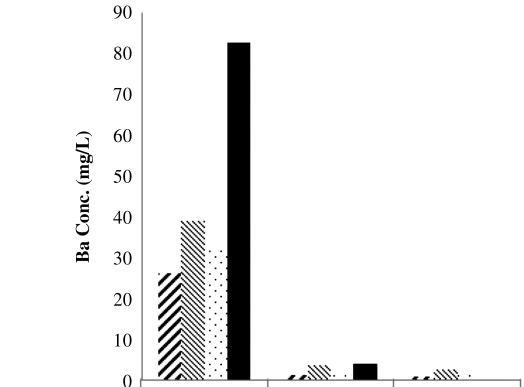

	150 mg/L sulfate	500 mg/L sulfate	1,000 mg/L sulfate
Davis	26.1	1.1	0.8
Wateq	38.8	3.5	2.6
Pitzer	32.6	2.2	1.6
Measurement	82.5	3.8	0

(a)

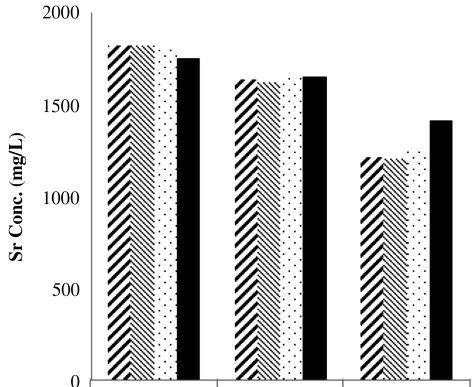

	150 mg/L sulfate	500 mg/L sulfate	1,000 mg/L sulfate
Davis	1,812	1,629	1,209
Wateq	1,812	1,617	1,202
Pitzer	1,812	1,645	1,236
Measurement	1,747	1,649	1,409

(b)

Fig. 5. Comparison between equilibrium predictions and experimental results for different initial sulfate concentrations after 24 h of reaction in synthetic flowback water from Site C for (a) Ba; (b) Sr

organics such as commercial antiscalants and polyphosphonates could retard precipitation reactions even if present at very low concentrations (Van der Leeden 1991). However, some other organics like methanol could promote the precipitation reactions (Jones et al. 2008).

The kinetics and equilibrium of barite and celestite precipitation in actual flowback water were evaluated using actual flowback water from Site A. The main difference between actual and synthetic flowback water is that the actual flowback water contains organic matter, with total organic carbon concentration of 52 mg/L. It was found that Ba concentration reached equilibrium after 30 min reaction in actual flowback water for all sulfate doses evaluated in this study (data not shown), which is identical to the behavior observed in the synthetic flowback water. As shown in Fig. 6, the measured Ba concentration at equilibrium deviated from model predictions for the initial sulfate dose of 400 mg/L. Higher Ba concentration in solution at equilibrium is likely due to an increase in barite solubility in the presence of organic matter (Church and Wolgemuth 1972). This study revealed that organic matter does not have any observable impact on barite precipitation kinetics (data not shown). However, chemical-equilibrium models tend to overestimate Ba removal in actual flowback water because the impact of organic matter cannot be adequately incorporated into thermodynamic calculations.

Fig. 7 illustrates the difference in celestite precipitation kinetics in actual and synthetic flowback water from Site A. Fig. 7 shows that celestite precipitation is slower in actual flowback water compared with that in synthetic flowback water, which is due to inhibition by organic matter present in actual flowback water.

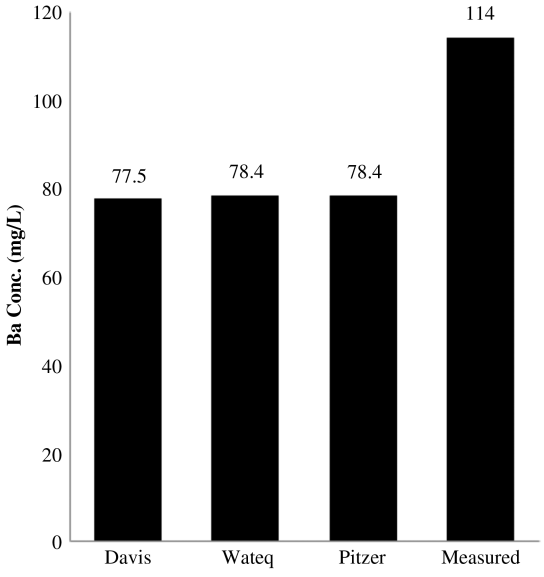

Fig. 6. Comparison between equilibrium predictions and measured residual Ba concentration after 24 h of reaction in actual flowback water from Site A with 400 mg/L initial sulfate concentration

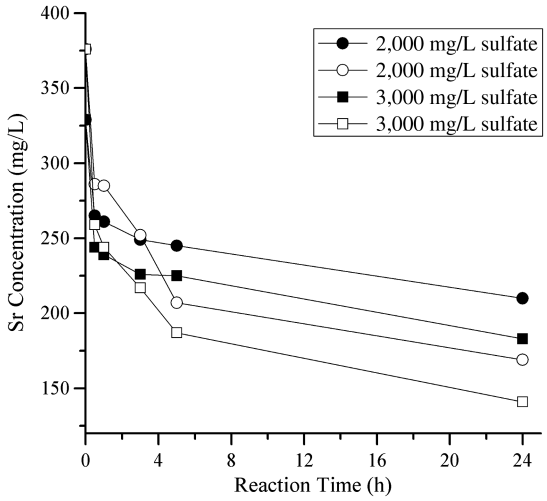

Fig. 7. Strontium concentration in synthetic (open symbols) and actual flowback water (solid symbols) from Site A during sulfate precipitation

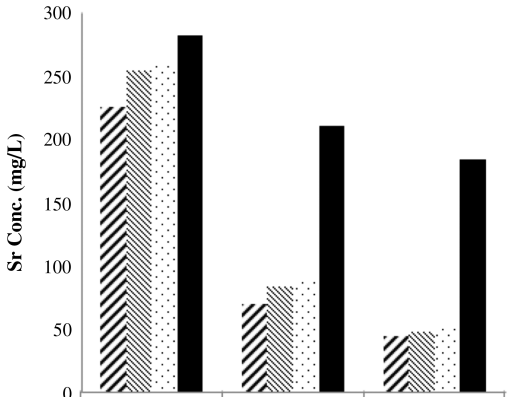

	1,000 mg/L sulfate	2,000 mg/L sulfate	3,000 mg/L sulfate
Davis	225	69	44.2
Wateq	254	83	47.6
Pitzer	261	88	51.4
Measured	282	210	183

Fig. 8. Comparison between equilibrium predictions and measured residual Sr concentration after 24 h of reaction in actual flowback water from Site A for different initial sulfate concentration

Adsorption of organic matter on active sites on the crystal surface could block the crystal growth and decrease the kinetics of precipitation reactions (Hamdona et al. 2010). This effect was previously identified for barium sulfate precipitation at low supersaturation ratios (Van der Leeden 1991). However, inhibition of barite precipitation by organic matter was not observed under the experimental conditions evaluated in this study (i.e., high ionic strength and high supersaturation ratio for barite) because the reaction was essentially completed in 30 min. In comparison, celestite precipitation is much slower, and further reduction in celestite precipitation kinetics caused by the organic matter present in the actual flowback water additionally exacerbated the difference between measured and predicted Sr concentrations (Fig. 8). Therefore, equilibrium models may not be reliable in predicting Sr concentration in centralized wastewater-treatment plants due to kinetic limitations.

Summary and Conclusions

Laboratory experiments were conducted to evaluate the kinetics of barite and celestite precipitation and associated Ba and Sr removal from flowback water through sulfate precipitation. It was found that barium reacted rapidly with sulfate and essentially reached equilibrium within 30 min. One exception was in the case of low initial Ba (236 mg/L) and sulfate (150 mg/L) concentrations, but moderate strontium concentration (1,817 mg/L). Reduction in the barium removal rate in this case was due to initial Ba and Sr coprecipitation with sulfate followed by slow substitution of Sr with Ba. Furthermore, barite precipitation may be inhibited in high ionic strength solutions and low barite saturation index.

Comparison between measured and predicted concentrations in synthetic flowback water solutions revealed that the chemical-equilibrium model based on the Pitzer equation for activity corrections was superior in predicting both Ba and Sr concentration because of the very high ionic strength that characterizes most flowback waters from unconventional gas extraction. Discrepancies between measured and predicted results, especially in the case of Sr, could be significant because of the slow celestite-precipitation rate. In that case, chemical-equilibrium models cannot reliably predict the quality of the effluent from central waste-treatment plants utilizing sulfate precipitation for the control of Ba and Sr. This study also suggests that sulfate may not the best agent for Sr removal from flowback water, and that other anions (e.g., carbonate) may be better suited to remove high levels of Sr.

Barite and celestite precipitation in actual flowback water may be influenced by the presence of natural and synthetic organic matter in this water. Although the organic matter had no observable impact on barite precipitation kinetics, the rate of celestite precipitation was significantly reduced. Deviations between measured and predicted Ba concentrations were influenced by the increase in barite solubility in the presence of organic matter. As the rate of celestite precipitation was reduced further in the actual flowback water, it would take even longer for Sr concentration to reach equilibrium compared to the results in synthetic flowback water. Therefore, chemical-equilibrium models may not be able to accurately predict the composition of effluent from centralized wastewater-treatment plants treating flowback water from unconventional gas production. Due to the complexity of organics that are present in flowback water, no specific compound can be singled out for its influence on the kinetics and equilibrium of barite and celestite precipitation.

References

Agilent Technologies. (2010). *Flame atomic absorption spectrometry: Analytical method*, 10th Ed., Agilent Technologies, Santa Clara, CA.

Aniceto, J. P., Cardoso, S. P., Faria, T. L., Lito, P. F., and Silva, C. M. (2012). "Modeling ion exchange equilibrium: Analysis of exchanger phase non-ideality." *Desalination*, 290(30), 43–53.

Barbot, E., Vidic, N., Gregory, K., and Vidic, R. D. (2013). "Spatial and temporal correlation of water quality parameters of produced waters from Devonian-age shale following hydraulic fracturing." *Environ. Sci. Technol.*, 47(6), 2562–2569.

Burkin, A. R. (2001). *Chemical hydrometallurgy: Theory and principles*, Imperial College Press, London, U.K.

Church, T. M., and Wolgemuth, K. (1972). "Marine barite saturation." *Earth Planet Sci Lett.*, 15(1), 35–44.

Davis, C. W. (1962). *Ion association*, Butterworths, London.

de Witt, W. (1993). "Principal oil and gas plays in the Appalachian basin (Province 131)." *U.S. Geological Survey Bulletin 1839-I*, U.S. Geological Survey, Washington, DC.

Economides, M. J., Watters, L. T., and Dunn-Norman, S. (1998). *Petroleum well construction*, John Wiley & Sons, West Sussex, England.

Engelder, T., and Lash, G. G. (2008). "Marcellus shale play's vast resource potential creating stir in Appalachia." *Am. Oil Gas Reporter*, 51(6), 76–87.

EPA. (1974). "Methods for the chemical analysis of water and wastes." *EPA/600/4-79/020*, U.S. Environmental Protection Agency, Washington, DC.

Fan, C., Kan, A. T., Zhang, P., and Tomson, M. B. (2011). "Barite nucleation and inhibition at 0 to 200°C with and without thermodynamic hydrate inhibitors." *SPE J.*, 16(2), 440–450.

Greenberg, J. P., and Moller, N. (1989). "The prediction of mineral solubilities in natural water: A chemical equilibrium model for the Na-K-SO_4-H_2O system to high concentrations from 0 to 250°C." *Geochim. Cosmochim. Acta*, 53(10), 2,503–2,518.

Hamdona, S. K., Hamza, S. M., and Mangood, A. H. (2010). "The influence of polyphosphonates on the precipitation of strontium sulfate (celestite) from aqueous solutions." *Desalination Water Treat.*, 24(1–3), 55–60.

Harper, J. A. (2008). "The Marcellus shale: An old new gas reservoir in Pennsylvania." *Penn. Geol.*, 38(1), 2–13.

Harvie, C. E., Moller, N., and Weare, J. H. (1984). "The prediction of mineral solubilities in natural waters: The Na-K-Mg-Ca-H-Cl-SO_4-OH-HCO_3-CO_3-CO_2-H_2O system to high ionic strength at 25°C." *Geochim. Cosmochim. Acta*, 48(4), 723–751.

J. Environ. Eng.

He, S., Oddo, J. E., and Tomson, M. B. (1995a). "The nucleation kinetics of barium sulfate in NaCl solutions up to 6 M and 90°C." *J. Colloid Interface Sci.*, 174(2), 319–326.
He, S., Oddo, J. E., and Tomson, M. B. (1995b). "The nucleation kinetics of strontium sulfate in NaCl solutions up to 6 M and 90°C with or without inhibitors." *J. Colloid Interface Sci.*, 174(2), 327–335.
Hennesy, A. J. B., and Graham, G. M. (2002). "The effect of additives on the co-crystallisation of calcium with barium sulfate." *J. Cryst. Growth*, 237–239(3), 2153–2159.
Hill, D. G., Lombardi, T. E., and Martin, J. P. (2004). "Fractured shale gas potential in New York." *Northeastern Geol. Environ. Sci.*, 26(1/2), 57–78.
Holmes, H. F., Baes, C. F. B. Jr., and Mesmer, R. E. (1987). "The enthalpy of dilution of HCl(aq) to 648 K and 40 MPa: Thermodynamic properties." *J. Chem. Therm.*, 19(8), 863–890.
Jones, F., Oliviera, A., Parkinson, G. M., Rohl, A. L., Stanley, A., and Upson, T. (2004). "The effect of calcium ions on the precipitation of barium sulfate 1: Calcium ions in the absence of organic additives." *J. Cryst. Growth*, 262(1–4), 572–580.
Jones, F., Piana, S., and Gale, J. D. (2008). "Understanding the kinetics of barium sulfate precipitation from water and water-methanol solutions." *Cryst. Growth Des.*, 8(3), 817–822.
Merkel, B. J., and Planer-Friedrich, B. (2008). *Groundwater geochemistry: A practical guide to modeling of natural and contaminated aquatic systems*, 2nd Ed., Springer-Verlag, Berlin.
Milici, R. C., and Swezey, C. S. (2006). *Assessment of Appalachian basin oil and gas resources: Devonian Shale–middle and upper Paleozoic total petroleum system*, U.S. Department of the Interior, U.S. Geological Survey, Reston, VA.
Miller, C. W., and Benson, L. V. (1983). "Simulation of solute transport in a chemically reactive heterogeneous system: Model development and application." *Water Resour. Res.*, 19(2), 381–391.
Monnin, C. (1999). "A thermodynamic model for the solubility of barite and celestite in electrolyte solutions and seawater to 200°C and to 1 kbar." *Chem. Geol.*, 153(1), 187–209.
Monnin, C., and Galinier, C. (1988). "The solubility of celestite and barite in electrolyte solutions and natural waters at 25°C: A thermodynamic study." *Chem. Geol.*, 71(4), 283–296.
Pabalan, R. T., and Pitzer, K. S. (1987). "Thermodynamics of concentrated electrolyte mixtures and the prediction of mineral solubilities to high temperatures for mixtures in the system Na-K-Mg-Cl-SO_4-OH-H_2O." *Geochim. Cosmochim. Acta*, 51(9), 2429–2443.
Parkhurst, D. L., and Appelo, C. A. J. (1999). "User's guide to PHREEQC (version 2): A computer program for speciation, batch-reaction, one-dimensional transport, and inverse geochemical calculations." *U.S. Geological Survey, Water Resources Investigations Rep., 99-4259*, Washington, DC.
Parkhurst, D. L., Thorstenson, D. C., and Plummer, L. N. (1980). "PHREEQE: A computer program for geochemical calculations." *U.S. Geological Survey, Water Resources Investigations Rep., 80-96*, Washington, DC.
Pina, C. M., and Putnis, A. (2002). "The kinetics of nucleation of solid solutions from aqueous solutions: A new model for calculating non-equilibrium distribution coefficients." *Geochim. Cosmochim. Acta*, 66(2), 185–192.
Pitzer, K. S. (1973). "Thermodynamics of electrolytes. I Theoretical basis and general equations." *J. Phys. Chem.*, 77(2), 268–277.
Pitzer, K. S. (1975). "Thermodynamics of electrolytes. V. Effects of higher-order electrostatic terms." *J. Solution Chem.*, 4(3), 249–265.
Pitzer, K. S. (1991). *Activity coefficients in electrolyte solutions*, 2nd Ed., CRC, Boca Raton, FL.
Pitzer, K. S., and Kim, J. J. (1974). "Thermodynamics of electrolytes. IV. Activity and osmosis coefficients for mixed electrolytes." *J. Am. Chem. Soc.*, 96(18), 5701–5707.
Pitzer, K. S., and Mayorga, G. (1973). "Thermodynamics of electrolytes. II. Activity and osmotic coefficients for strong electrolytes with one or both ions univalent." *J. Phys. Chem.*, 77(19), 2300–2308.
Pletcher, J. (2008). "Drillers access mile-deep gas deposits in what may be new 'gold rush'." Herald Standard, Uniontown, PA.
Risthaus, P., Bosbach, D., Becker, U., and Putnis, A. (2001). "Barite scale formation and dissolution at high ionic strength studied with atomic force microscopy." *Colloid. Surface Physicochem. Eng. Aspect.*, 191(3), 201–214.
Rodgers, M., et al. (2008). "Marcellus shale: What local government officials need to know." Penn State Extension, College of Agricultural Sciences, Marcellus Education, University Park, PA.
Shen, D., Fu, G., Al-Saiari, H. A., Kan, A. T., and Tomson, M. B. (2009). "Barite dissolution/ precipitation kinetics in porous media and in the presence and absence of a common scale inhibitor." *SPE J.*, 14(3), 462–471.
Shen, D., Fu, G., Kan, H. A., and Tomson, M. B. (2008). "Seawater injection, inhibitor transport, rock-brine interactions, and $BaSO_4$ scale control during seawater injection." *SPE Int. Oilfield Scale Conf.*, Society of Petroleum Engineers, Richardson, TX.
Smith, E., Hamilton-Taylor, J., William, D., Fullwood, N. J., and McGrath, M. (2004). "The effect of humic substances on barite precipitation-dissolution behaviour in natural and synthetic lake waters." *Chem. Geol.*, 207(1–2), 81–89.
Truesdell, A. H., and Jones, B. F. (1974). "WATEQ, a computer program for calculating chemical equilibria of natural waters." *J. Res. US Geol. Sur.*, 2(2), 233–274.
Van der Leeden, M. C. (1991). "The role of polyelectrolytes in barium sulfate precipitation." Ph.D. dissertation, Technical Univ. of Delft, Delft, The Netherlands.
Vidic, R. D., Brantley, S. L., Vandenbossche, J. M., Yoxtheimer, D., and Abad, J. D. (2013). "Impact of shale gas development on regional water quality" *Science*, 340(6134), 1235009.
Westall, J. C., Zachary, J. L., and Morei, F. M. (1976). "MINEQL: A computer program for the calculation of chemical equilibrium composition of aqueous systems." *Technical Note No.18*, Ralph M. Parsons Laboratory, Massachusetts Institute of Technology, Cambridge, MA.
Yeboah, Y. D., Saeed, M. R., and Lee, A. K. K. (1994). "Kinetics of strontium sulfate precipitation from aqueous electrolyte solutions." *J. Cryst. Growth*, 135(1–2), 323–330.